Regulation of perforin activation and pre-synaptic toxicity through C-terminal glycosylation

Imran G House[1,2,†], Colin M House[1,†], Amelia J Brennan[1,2], Omer Gilan[2,3], Mark A Dawson[2,3,4,5], James C Whisstock[6,7], Ruby HP Law[6,7], Joseph A Trapani[1,2] & Ilia Voskoboinik[1,2,*] (iD)

Abstract

Perforin is a highly cytotoxic pore-forming protein essential for immune surveillance by cytotoxic lymphocytes. Prior to delivery to target cells by exocytosis, perforin is stored in acidic secretory granules where it remains functionally inert. However, how cytotoxic lymphocytes remain protected from their own perforin prior to its export to secretory granules, particularly in the Ca^{2+}-rich endoplasmic reticulum, remains unknown. Here, we show that N-linked glycosylation of the perforin C-terminus at Asn549 within the endoplasmic reticulum inhibits oligomerisation of perforin monomers and thus protects the host cell from premature pore formation. Subsequent removal of this glycan occurs through proteolytic processing of the C-terminus within secretory granules and is imperative for perforin activation prior to secretion. Despite evolutionary conservation of the C-terminus, we found that processing is carried out by multiple proteases, which we attribute to the unstructured and exposed nature of the region. In sum, our studies reveal a post-translational regulatory mechanism essential for maintaining perforin in an inactive state until its secretion from the inhibitory acidic environment of the secretory granule.

Introduction

The pore-forming protein, perforin, arms cytotoxic lymphocytes (CLs), made up of natural killer cells and cytotoxic T lymphocytes, with the capacity to eliminate virus-infected and/or cancerous cells. Perforin and pro-apoptotic serine proteases, granzymes, are stored in cytotoxic secretory granules that, upon formation of an immunological synapse with a target cell, are released by the CLs into the synaptic cleft [1–3]. There, perforin monomers bind to the target cell membrane through the Ca^{2+}-dependent C2 domain and oligomerise to form transmembrane pores on the target cell membrane [1,4]. These pores allow for the passive diffusion of granzymes into the target cell and the subsequent induction of apoptosis [5]. In humans, failure to deliver functional perforin by CLs due to bi-allelic mutations of the perforin gene or genes critical for perforin secretion results in the development of fatal immunoregulatory disease and/or cancer, demonstrating the paramount importance of perforin-mediated CL function for human survival [6–8].

Upon activation, CLs rapidly generate and store large quantities of perforin and granzymes. Granzymes are synthesised as zymogens and are activated by cathepsins C/H within cytotoxic secretory granules, where they have no access to their apoptotic substrates and cannot kill the host cell [9–12]. Similarly, once delivered to secretory granules, low pH renders perforin inactive [13]. However, how CLs safely synthesise and store perforin prior to its delivery to secretory granules is unknown.

It has been suggested that the heavily glycosylated and abundant glycoprotein serglycin may form complexes with perforin and negatively regulate its function within the secretory granules of the host cell [14]. However, recent studies with CTL/NK cells of serglycin-deficient mice provided little evidence to support this idea [15]. Moreover, it has been hypothesised that ~12–20 residues at the extreme C-terminus of perforin (residues 535–555, including an N-linked glycan at residue Asn549) could interfere with Ca^{2+}-binding to the C2 domain [16]. As a result, proteolytic cleavage of perforin's C-terminus within secretory granules was considered necessary to activate the protein prior to its release into the synaptic cleft. However, structural studies reveal that this region is spatially distant from the lipid and Ca^{2+}-binding site of the C2 domain, suggesting that a C-terminus/C2 domain interaction is unlikely [17,18]. In addition, full-length recombinant perforin generated in insect cells with an intact C-terminus has indistinguishable lytic

1 Cancer Immunology Program, Peter MacCallum Cancer Centre, Melbourne, Vic., Australia
2 Sir Peter MacCallum Department of Oncology, University of Melbourne, Parkville, Vic., Australia
3 Cancer Research Division, Peter MacCallum Cancer Centre, Melbourne, Vic., Australia
4 Centre for Cancer Research, University of Melbourne, Melbourne, Vic., Australia
5 Department of Haematology, Peter MacCallum Cancer Centre, Melbourne, Vic., Australia
6 Department of Biochemistry and Molecular Biology, Monash University, Clayton, Vic., Australia
7 Australian Research Council Centre of Excellence in Advanced Molecular Imaging, Monash University, Clayton, Vic., Australia
*Corresponding author. Tel: +61 3 8559 7096; E-mail: ilia.voskoboinik@petermac.org
†These authors contributed equally to this work

activity to perforin engineered to lack the final 12 amino acids [19]. Overall, it remains unknown as to how and why C-terminal cleavage occurs and, most importantly, how CLs are protected from perforin.

Here, we show that glycosylation of the perforin C-terminus at residue Asn549 is key to inhibiting perforin activity by blocking oligomerisation of perforin monomers. Consequently, proteolytic removal of the C-terminus is required to remove the inhibitory glycan and to activate the protein. Furthermore, using extensive site-directed mutagenesis, we excluded the presence of a predominant consensus site for endo-proteolytic processing. Rather, we postulate that progressive trimming of the C-terminus is achieved by multiple lysosomal peptidases and/or carboxypeptidases, of which some, but not all, are cysteine proteases. We therefore conclude that the N-glycosylated C-terminus of perforin plays an essential role in protecting CLs from perforin cytotoxicity by preventing monomers from oligomerising into perforin pores prior to granule exocytosis.

Results and Discussion

The most abundant mature form of perforin ends at Leu542

The C-terminus of mature, processed perforin (prPRF) has never been precisely defined in any species, but was predicted on the basis of epitope mapping to occur 20 residues from the immature C-terminus [17]. To address this issue, we performed a mass spectrometric analysis of deglycosylated perforin immunoprecipitated from the human NK cell line KHYG1. The most abundant protein species we observed consistent with prPRF had a molecular mass of 57,865 Da, which was within one Da of the predicted mass of deglycosylated perforin terminating at residue Leu542 (expected mass of 57,863.95; Fig 1A, average theoretical expected masses are outlined in Table EV1). Multiple minor species corresponding to shorter or longer perforin molecules with C-termini at Gln540, Met541, Leu543 or Gly544 were also present. By contrast, the longest form of perforin had a mass of 59,188 Da, closely consistent with the expected mass of deglycosylated full-length perforin (flPRF), terminating at residue Trp555 (expected mass of 59,186.39 Da; Fig 1A). Importantly, the mass of every peak we identified was increased by 20 Da under reducing condition, reflecting complete reduction of all 10 intramolecular disulphide bonds in perforin. This finding also provided evidence that all the spectroscopic peaks we characterised were indeed perforin and not contaminants of a similar mass (Fig EV1). Consistent with these findings, perforin purified from primary IL-2-activated human NK cells of three healthy donors showed a predominant Leu542-terminating prPRF form as well as a less abundant species terminating at residue Gln540 (Fig 1B). However, owing to the scarcity of primary NK-derived perforin (in contrast to KHYG1 cell-derived perforin), we were unable to detect other minor prPRF species or flPRF (Fig 1B). Our results showing cleavage in the vicinity of residue Leu542 were consistent with the predictions of Uellner *et al* [16] but suggest that processing of perforin may occur at multiple sites.

Mapping the perforin cleavage site by site-directed mutagenesis

To define a possible site for perforin processing by a granule-bound endopeptidase, we next generated perforin variants in which single serine substitutions were introduced for each residue in a region spanning Gln540 to Gly548. These variants were retrovirally transduced into KHYG1 cells in which CRISPR/Cas9 had been used to abolish endogenous perforin expression altogether (Fig EV2). The same constructs were also introduced into rat basophilic leukaemia (RBL) cells, which lack perforin expression but are capable of processing flPRF into an active form [20]. Despite these amino acid substitutions, every perforin variant we generated was processed similarly to WT-perforin in both cell lines (Figs 1C and D, and EV3). Surprisingly, we found that even simultaneously replacing every residue from Gln540 through to Gly548 with serine did not disrupt processing as we might have expected (Fig 1E). These findings excluded the possibility that the C-terminus contains a consensus site recognised by a single endopeptidase responsible for C-terminal processing. Mass spectrometric analysis of the same set of variants showed the C-terminus of prPRF to be similar to WT-perforin, typically at residue 542 (Fig 2A–C) or 541 (Fig 2D) or 543 (Fig 2E and F), depending on the mutation. These results indicate that introduction of single/multiple successive serine residues in the tail of perforin had minimal effect on perforin processing. In the absence of a consensus endopeptidase cleavage site, we concluded that the C-terminal peptide is processed by either multiple endopeptidases and/or carboxypeptidases. This hypothesis is supported by data derived from the X-ray crystal structure of mouse perforin, whereas residues 542–554 are unstructured and not visible in electron density, residues Leu541 and Gly540 (Leu542 and Met541 in human perforin, respectively) interact intimately with the backbone of the molecule through main chain interactions. Moreover, all residues to the N-terminal side of Leu541 are buried and predicted to be far less easily accessible to proteases (Fig 2G).

Figure 1. Processed perforin exhibits multiple C-termini.

A   Perforin was immunoprecipitated from the human NK cell line KHYG1 and, following deglycosylation with PNGaseF and reduction with DTT, was analysed by mass spectrometry. Peaks consistent with perforin are annotated with mass observed and predicted carboxy-terminal residue. Data shown are the average of six independent experiments (individual MS spectra of perforin from untreated and DMSO-treated cells are shown in Appendix Fig S1).

B   Perforin from IL-2-stimulated primary NK cells from three healthy donors was prepared and analysed as above.

C, D   Perforin variants harbouring single amino acid substitutions spanning Gln540–Gly548 were expressed in a perforin knockout KHYG1 and/or RBL cells (summarised in D). Perforin expression and processing of serine-substituted mutants was assessed by Western blot; shown is a representative of three replicate experiments in KHYG1 cells.

E   Perforin variants harbouring multiple serine substitutions in the region from Gln540 to Gly548 (as illustrated within the figure) were expressed and assessed for expression and processing as per (C).

Data information: "flPRF", full-length (unprocessed) perforin; "prPRF", processed (truncated perforin); HSP90, heat-shock protein 90 (loading control).
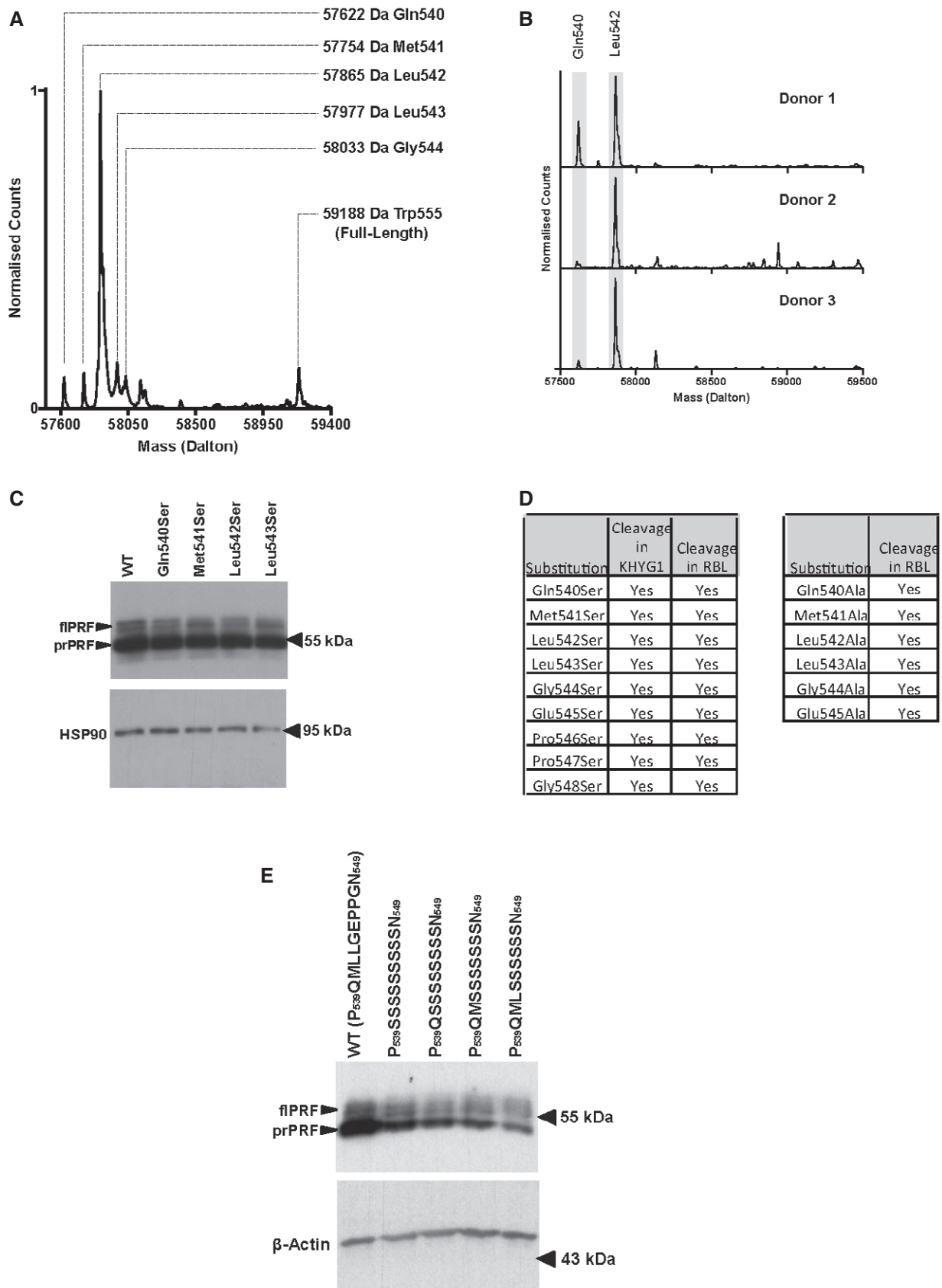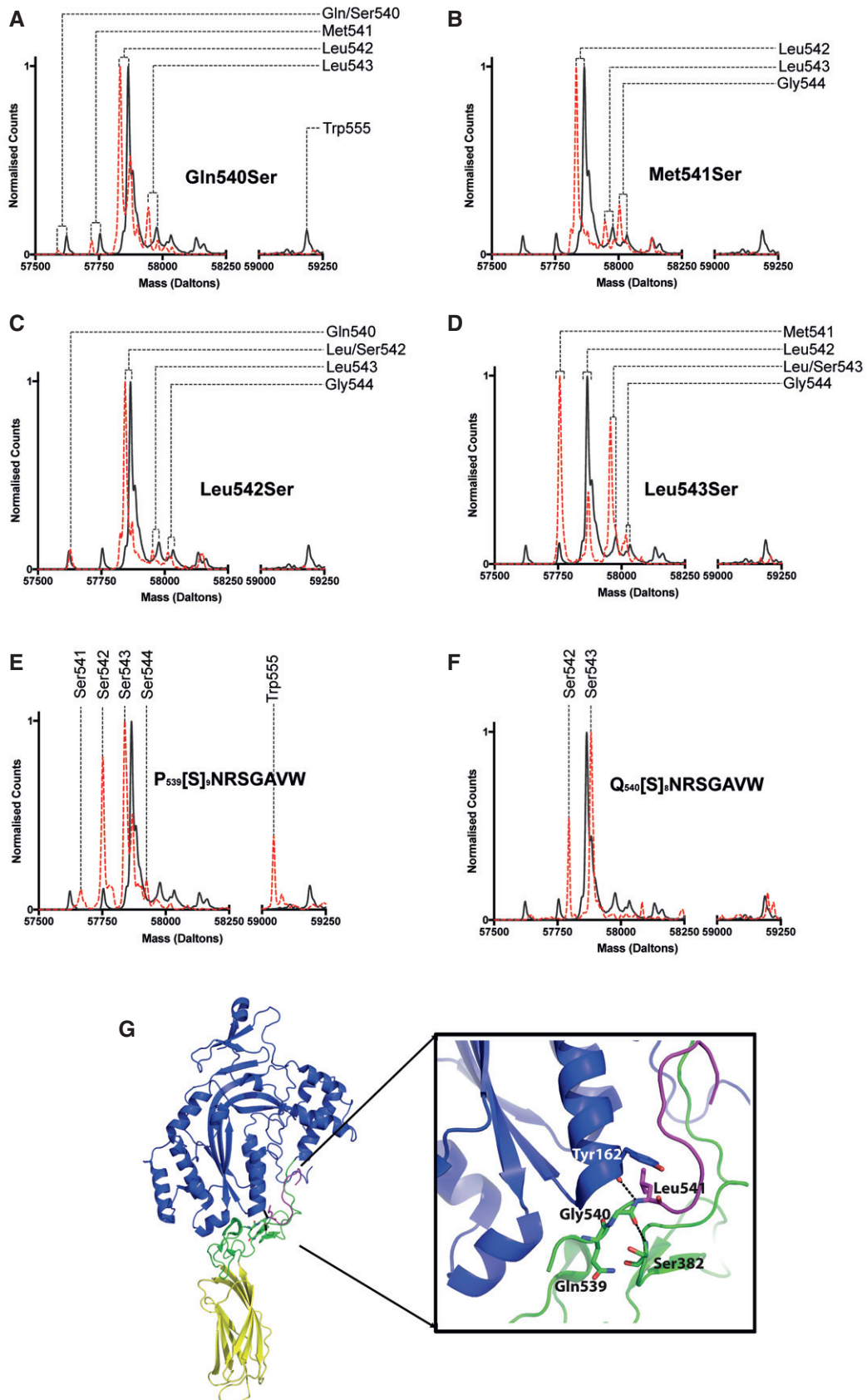
Figure 1.

Figure 2.

◄

Figure 2. Perforin is processed in close proximity to residue 542, irrespective of the C-terminal sequence.

A–F   Perforin variants harbouring mutations (A) Gln540Ser, (B) Met541Ser, (C) Leu542Ser, (D) Leu543Ser or multiple serine substitutions from (E) Gln540–Gly548 or (F) Met541–Gly548 were expressed in and immunoprecipitated from a perforin knockout KHYG1 cell line and perforin processing was assessed by mass spectrometry. All peaks are shown as a representative of two independent experiments. Shown in black trace is the average of six independent untreated controls that are also shown in Fig 1A.

G   Cartoon representation of X-ray crystal structure of mouse perforin (PDB ID 3NSJ) showing MACPF (blue), shelf (green), C2 (yellow) and the C-terminal region (residues 541–551, magenta). Also shown are the main chain interactions between Leu541 (Leu542 in human perforin) and Tyr162, and between Gly540 (Met541 in human perforin) and Ser382 (dotted lines).

Carboxy-terminal N-linked glycan inhibits perforin function

We next compared the cytolytic function of WT prPRF (lacking the C-terminal residues and associated glycan) and flPRF, over-expressed in our perforin knockout KHYG1 cell line. It has previously been shown that perforin C-terminal processing is highly dependent on the acidic pH of cytotoxic granules [16], so we enriched flPRF from KHYG1 cells in which granule pH was neutralised with the H^+-ATPase inhibitor concanamycin A (CNCA). This approach allowed us to directly assess the cytotoxicity of isolated flPRF and eliminated potential off-target effects of CNCA treatment on NK cell function. Western blot and mass spectrometry confirmed that perforin from CNCA-treated cells was full-length and glycosylated at the C-terminus, whereas greater than 80% of the perforin enriched from DMSO-treated KHYG1 cells (control) was cleaved at the C-terminus (lacking the C-terminal glycan; Fig 3A and B). Strikingly, flPRF had minimal lytic activity, demonstrating that glycosylated flPRF generated in mammalian cells was not cytolytic (Fig 3C).

We next repeated these experiments with the membrane-soluble cysteine protease inhibitor E64D, which was previously shown to reduce, but not totally abolish perforin C-terminal processing [16]. Western blot analysis of perforin isolated from E64D-treated KHYG1 cells showed a $36 \pm 14\%$ SD ($n = 3$) reduction in the amount of cleaved perforin compared to control (DMSO-)-treated cells ($P < 0.02$; Fig 3D). Mass spectrometry confirmed that E64D mostly inhibited processing to residue Leu542, but interestingly did not inhibit processing of perforin's most C-terminal residues (Val554 and Trp555), presumably by a non-cysteine protease (Fig 3E). Nevertheless, consistent with the reduction of prPRF on Western blot, perforin isolated from E64D-treated cells was $41.0 \pm 1.5\%$ SD ($n = 3$) less cytotoxic than perforin from DMSO-treated cells ($P < 0.001$; Fig 3F), further demonstrating that perforin with an intact glycosylated C-terminus is indeed non-lytic.

Despite considerable sequence divergence at the C-terminus of perforin between mammals and marsupials, and other vertebrates, the C-terminal N-linked glycosylation has remained a common feature, indicating a likely conservation of function (Fig EV4). We therefore investigated whether the lack of lytic function of full-length perforin is due to the presence of glycan at this site. To study this, prPRF and flPRF enriched from KHYG1 cells were treated with PNGaseF (an asparagine amidase that removes all N-linked glycans), EndoH (which specifically removes N-linked high-mannose carbohydrate from moieties typically added to proteins in the ER) or neuraminidase (which removes negatively charged terminal sialic acid from complex glycans). Strikingly, EndoH and PNGaseF treatment resulted in a > 10 increase in flPRF lytic activity while neuraminidase had no effect (Fig 4A). By comparison, the

function of prPRF did not change significantly with any glycosidase (Fig 4A). These data demonstrate that removal of both complex and high-mannose glycans attached at Asn549 results in perforin activation.

Human perforin encodes two N-linked glycosylation sites at residues Asn205 and Asn549. To confirm that recovery of perforin function was due to C-terminal deglycosylation at Asn549 (and not at Asn205), we expressed a perforin variant harbouring mutation Asn549Gln (and hence lacked C-terminal glycosylation) in perforin-deficient KHYG1 cells. As Asn549Gln-perforin is toxic and has reduced expression [19], we were unable to enrich sufficient amounts of the mutant to perform assays following CNCA treatment, which further reduces perforin expression in KHYG1 cells. Instead, we enriched perforin from Asn549Gln-expressing cells treated with E64D and found that despite inhibition of processing at the C-terminus, there was no loss of function compared to perforin from DMSO-treated cells ($5.0 \pm 11.2\%$ SD, $n = 3$, $P = 0.5$; Fig 4B). These data were in stark contrast to experiments performed with WT-perforin (Fig 3F) and confirmed that the C-terminal glycan regulates perforin cytotoxicity.

Mechanism of perforin inhibition by the C-terminal glycan

Previously, it was suggested that the C-terminal glycan interfered with the perforin C2 domain and, consequently, reduced membrane binding [16]. To assess directly whether the C-terminal glycan regulates Ca^{2+}-dependent membrane binding, we assessed the capacity of purified prPRF (from untreated KHYG1), flPRF (from CNCA-treated KHYG1) or perforin isolated from E64D-treated cells, to bind to the cell membrane at 4°C, which is permissible for membrane binding, but not oligomerisation or lysis. We found that flPRF and prPRF bound the plasma membrane equally well and in a Ca^{2+}-dependent manner (Fig 4C).

In the absence of evidence for reduced membrane binding, we next considered the effect of C-terminal glycosylation on perforin oligomerisation. We have previously shown that oligomerised and membrane-inserted perforin does not readily disassemble to the monomeric form, and this is manifested as a loss of monomeric perforin on SDS–PAGE; however, monomers are recovered following treatment with 8 M urea [4]. Therefore, perforin enriched from DMSO- or CNCA-treated KHYG1 cells was incubated with red blood cells at 37°C for 20 min to allow for perforin oligomerisation and membrane insertion. This resulted in loss of prPRF monomer, but not flPRF, however, the prPRF monomer signal was restored following denaturation with urea (Fig 4D and E). To formally demonstrate that inhibition of oligomerisation was dependent on the C-terminal glycan, we repeated the experiment with Asn549Gln-perforin. We found an absence of both full-length and
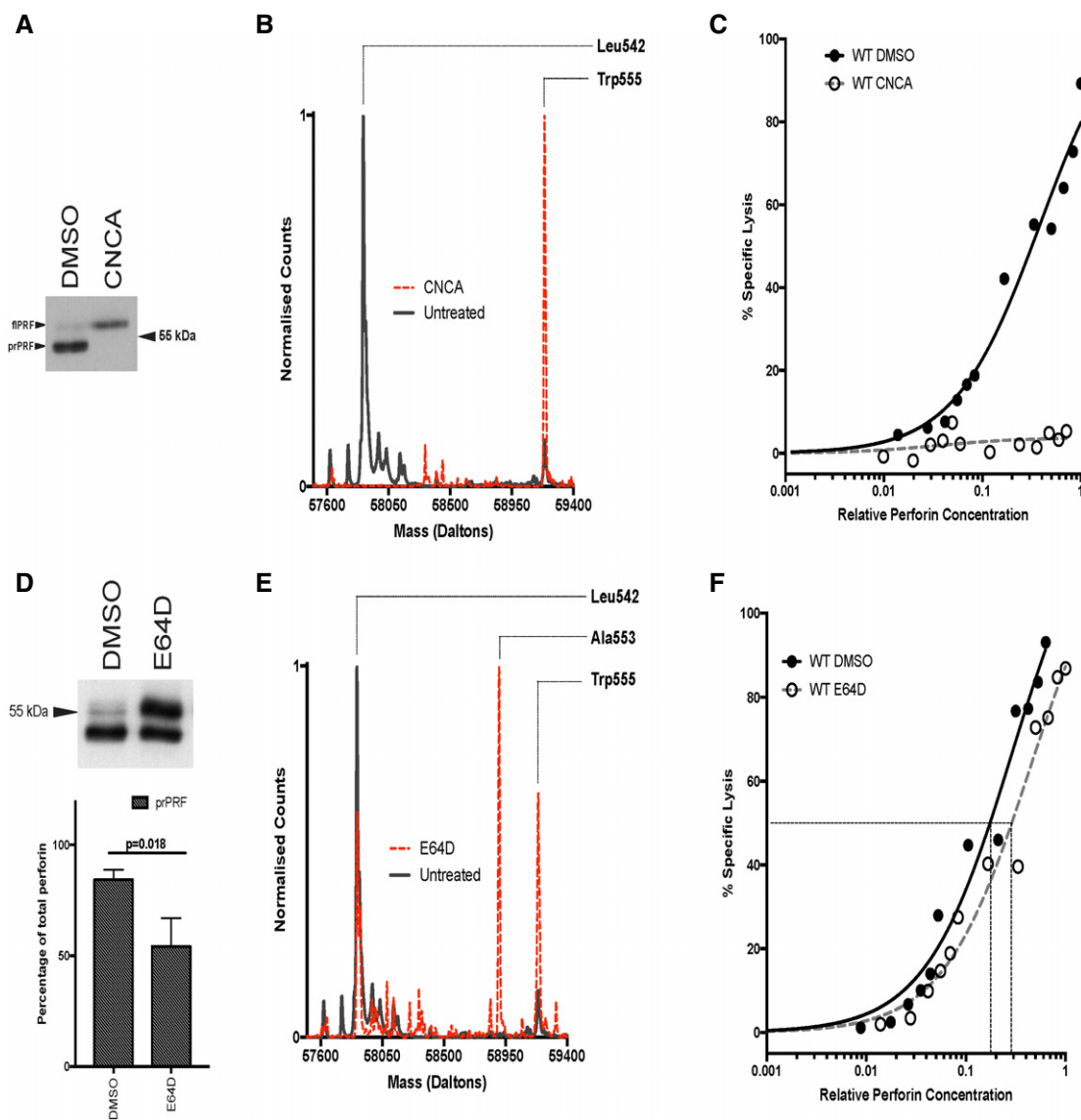
Figure 3. Full-length perforin with an intact glycosylated carboxy-terminus is not cytolytic.

A, B   Perforin isolated from KHYG1 cells treated with 25 ng/ml CNCA was assessed by (A) Western immunoblotting or (B) mass spectrometry (shown is a representative of two independent experiments compared to the average of six independent untreated controls that are also shown in Fig 1A and Appendix Fig S1).

C   The cytolytic potential of IMAC-enriched perforin from DMSO- or CNCA-treated KHYG1 cells was assessed in a 1-h ^{51}Cr-release assay using K562 target cells. Shown is a representative of three independent experiments.

D   Perforin cleavage in KHYG1 cells treated with 20 μM E64D was assessed by Western blot analysis. Shown as a bar graph is the quantification of prPRF as a percentage of total perforin in KHYG1 cells after DMSO or E64D treatment, from three independent experiments (shown is mean ± SD). Perforin from E64D-treated cells showed a statistically significant reduced level of prPRF (*P* = 0.018) as assessed by unpaired *t*-test.

E   Perforin was immunoprecipitated from E64D-treated cells and analysed by mass spectrometry. Shown is a representative of two independent experiments compared to the average of six independent untreated controls that are also shown in Fig 1A.

F   The function of perforin isolated from E64D-treated cells was assessed in a 1-h ^{51}Cr-release assay using K562 target cells. Shown is a representative experiment of three independent experiments (individual experiments are shown in Appendix Fig S2A). Perforin isolated from E64D-treated cells was 41.0 ± 1.5% SD (*n* = 3) less cytotoxic than perforin from DMSO-treated cells (*P* = 0.0007, ratio paired *t*-test). The dashed lines on the graph represent the relative amount of perforin required to achieve 50% maximal lysis.

processed monomeric perforin after 20 min of incubation with target cells (Fig 4F), but both signals were recovered with urea treatment. Together, these data demonstrate that the glycan at Asn549 inhibits the oligomerisation of perforin, and that its removal is essential for pore formation.

Major surprises and concluding remarks

One key question remaining in cytotoxic lymphocyte biology is how they safely synthesise and store one of the most cytotoxic yet essential elements of the immune system, perforin. This
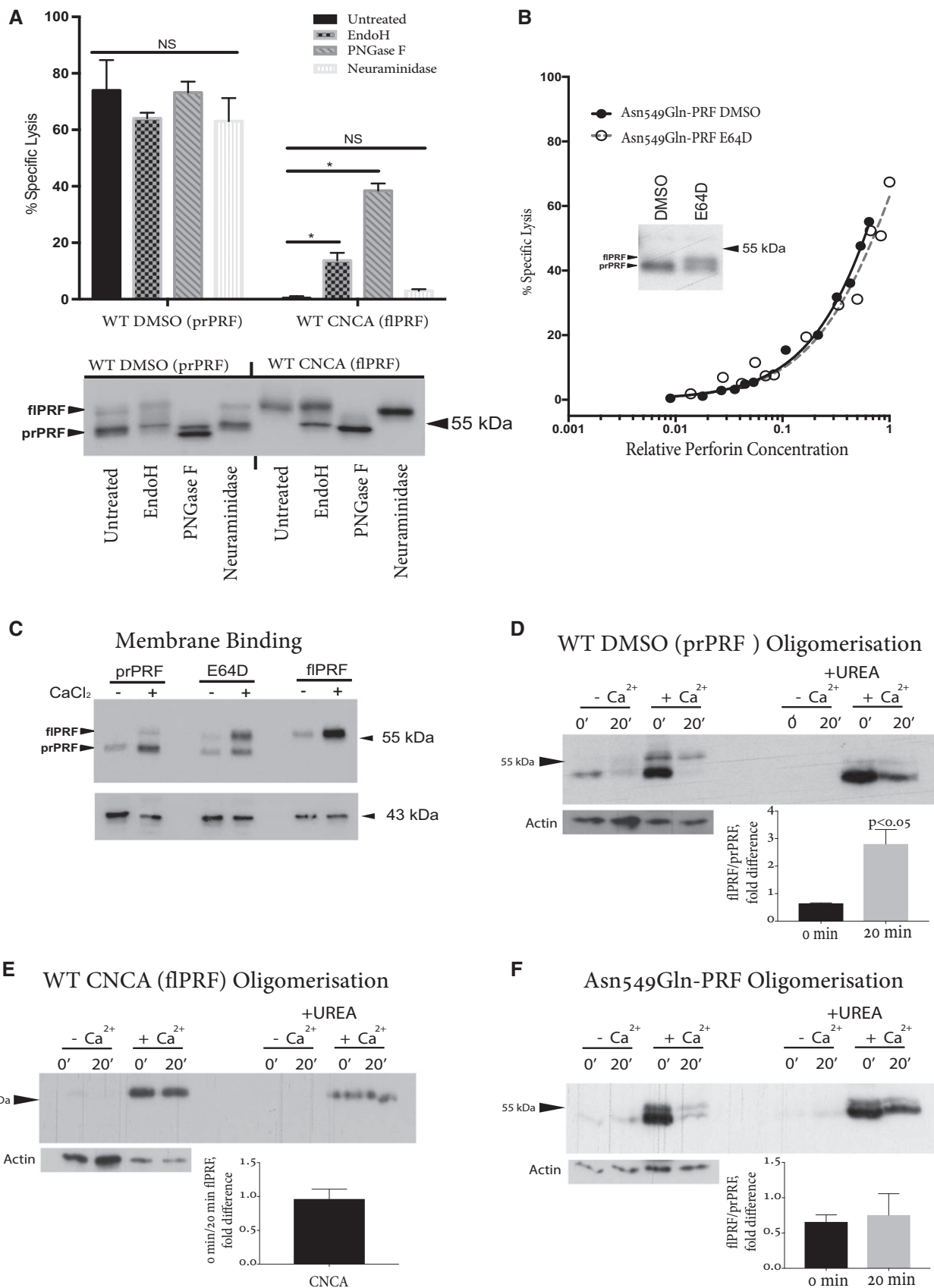
Figure 4.

Figure 4. C-terminal glycosylation inhibits perforin oligomerisation.

A   Perforin isolated from DMSO- or CNCA-treated cells was treated with EndoH, PNGaseF or neuraminidase for 20 min at room temperature and assessed for function in a 1-h ^{51}Cr-release assay using K562 target cells. *$P < 0.05$ as assessed by multiple comparisons two-way ANOVA (individual experiments are shown in Appendix Fig S2B)

B   Asn549Gln variant of perforin (the C-terminal glycosylation site mutant) was expressed in perforin knockout KHYG1 cells; the cells were treated with either DMSO or 20 μM E64D, the mutant perforin isolated and assessed for lytic potential as above. Shown is a representative of three independent experiments (individual experiments are shown in Appendix Fig S2C). The function of Asn549Gln perforin was not affected by E64D treatment ($5 \pm 11.2\%$ SD, $n = 3$, $P = 0.48$, ratio paired *t*-test). Shown inset is a representative of Western blot of Asn549Gln perforin after DMSO and E64D treatment.

C   Perforin isolated from KHYG1 cells treated with either DMSO, E64D or CNCA was bound to sheep red blood cells (SRBCs) +/− CaCl$_2$ at 4°C for 2 min. SRBCs were then solubilised and assessed for perforin binding by Western blot analysis.

D–F Perforin isolated from DMSO-treated KHYG1 cells was incubated with SRBCs for 20 min at 37°C (D) to allow for perforin to oligomerise. Perforin oligomerisation was then assessed by Western blot analysis, where samples were solubilised with or without 8 M urea. This experiment was repeated with (E) full-length perforin from CNCA-treated cells and (F) Asn549Gln-perforin. Shown are representative experiments of three independent replicates. The Western blots from three independent experiments were quantified, and bar graphs in (D) and (F) show the ratio of flPRF (an upper band) and prPRF (a lower band) at 0 min or at 20 min (mean $\pm$ SEM, $n = 3$). Statistical significance ($P < 0.05$) was determined by unpaired *t*-test with Welch's correction and arcsine transformation. In (E), in the absence of a lower band, we measured a ratio between the intensity of upper bands at 0 and 20 min (0.96 ± 0.08, mean $\pm$ SEM, $n = 3$).

question is particularly pertinent within the ER where neutral pH and high Ca^{2+} concentrations allow perforin to exert its cytotoxicity within the host cell [19]. Here, we have uncovered a unique mechanism whereby a C-terminal glycan inhibits perforin oligomerisation and pore formation thus protecting the host from perforin cytotoxicity prior to its delivery to the cytotoxic secretory granules (Fig 5). Once within the granules, the C-terminal glycopeptide is proteolytically cleaved [16], but perforin remains inactive due to the acidic pH [13]. Once secreted into the synaptic cleft, the neutral pH and elevated Ca^{2+} concentration enable the proteolytically processed perforin to form pores in the target cell membrane.

Previously, we discovered that rapid export of perforin from the ER is a key component of CL protection and is critically reliant on the C-terminal region, in particular the final residue, Trp555 [19]. Similarly, we noted that although the mutation of glycosylated asparagine (Asn549Gln) does not disrupt ER export, high levels of expression of the mutant perforin result in death of the host cell [19]. Thus, in concert, our recent and current studies have now shown that the C-terminal peptide of perforin protects CLs from its cytotoxicity by facilitating both rapid export from the ER (glycan-independent) and also by "silencing" function of the protein (glycan-dependent).

Our findings demonstrate that processing of the glycosylated C-terminus within the secretory granules is critical for preparing perforin for pore formation within the immune synapse. In turn, we have described a mechanism by which glycosylation is used to silence perforin function which, to our knowledge, is a rare example of glycosylation being used in this manner. We observed that perforin oligomerisation was effectively inhibited by both high-mannose (acquired in the ER) and complex glycans acquired in mammalian cells and that removal of charged sialic acids from these glycans with neuraminidase did not impact their ability to inhibit perforin function. Previously, we observed that when generated in insect cells, perforin with an intact C-terminal peptide had identical function to perforin lacking the peptide [19]. In the light of our current data, we can now attribute this observation to the smaller C-terminal glycan additions acquired in insect cells, which have no apparent effect on perforin activity. Our data therefore suggest that inhibition of function by the C-terminal glycan likely occurs through steric hindrance of

oligomerisation. Indeed, it has been well documented [21] that a major difference between recombinant proteoglycans expressed in *Spodoptera frugiperda* and mammalian cells is a substantial trimming of the N-linked glycans in the insect cells to Man$_3$GlcNac$_2$ [21]. Given that our recombinant perforin remains fully functional, despite being glycosylated [19], we postulate that three mannose structures do not provide sufficient steric hindrance to inhibit its activity; in contrast, up to nine mannose structures [21] added to endogenous perforin appear to be sufficient to protect the host cell from perforin oligomerisation and toxicity in the endoplasmic reticulum. This notion may explain why the regulation of protein function by glycosylation would likely be maintained despite the documented "microheterogeneity" in mammalian glycosylation patterns [22]. Remarkably, despite divergence in the sequence of the C-terminal peptide between mammals and marsupials, and lower order vertebrates, the glycosylation of the C-terminus has remained a common feature of that region (Fig EV4) suggesting that regulation of perforin function through glycosylation/deglycosylation of the C-terminus may be an evolutionary conserved feature of the molecule. Moreover, cleavable carboxy-terminal peptides have been shown to play an important role in other pore-forming toxins [23,24], where they influence the solubility or the pore-forming activity of those bacterial virulence factors. The fact that a higher eukaryote perforin, despite its evolutionary divergence from ancestral bacterial toxins, also utilises C-terminal processing as a mechanism of activation is remarkable.

Despite the critical importance of perforin cleavage, we made the most surprising discovery that the C-terminus does not contain a predominant protease consensus cleavage residue, although hypothetically a nearby region may have a specific protease binding site. Indeed, we present data to suggest that the removal of the C-terminus is facilitated by lysosomal proteases that have the capacity to process the protein, irrespective of the amino acid sequence. Based on the previously solved X-ray crystal structure of perforin [17], we suggest that, due to a lack of either secondary structure or constraint and the surface exposure of the region, the C-terminus may be generally susceptible to proteolysis. This is consistent with the observation that processed perforin most commonly terminates at residue Leu542, which is the last C-terminal residue to make hydrogen bond contact with the backbone of
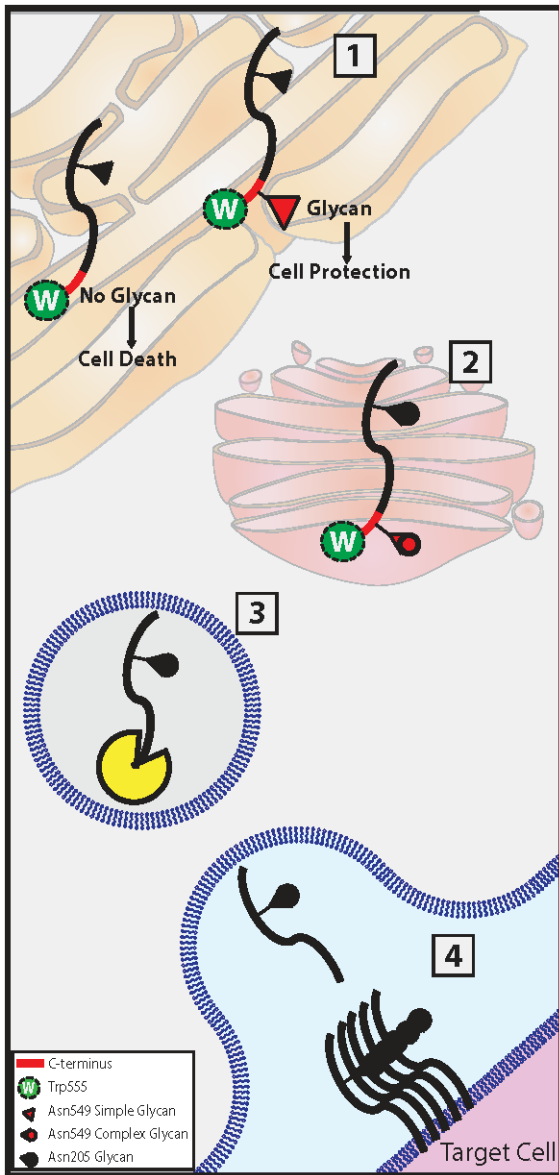
glycosidases that process the glycan and/or endopeptidases that process at the N-terminal side of Asn549. Indeed, one previous study suggested a role for cathepsin L and other cysteine proteases in perforin processing [25]. However, inhibiting even this entire class of diverse granule proteases had only a partial effect on perforin (and cytotoxic lymphocyte) function, thus supporting our current observations. We argue that, paradoxically, non-specific processing of the C-terminus may have evolved to avoid inhibition of perforin activation by viral peptides that could inhibit individual granule proteases.

With consideration of our study [19], we can here conclude that the N-glycosylated C-terminal peptide of perforin plays a critical role in protecting CLs from perforin cytotoxicity through two mechanisms: Trp555 and immediately adjacent residues facilitate perforin's rapid transit from the ER to the secretory granules, while the glycan situated at Asn549 inhibits perforin function by preventing monomers from oligomerising into pores prior to granule exocytosis. Our findings position the processing of the perforin C-terminus within secretory granules as critical to CL function and, in turn, immune homoeostasis.

Materials and Methods

Human primary NK cell isolation and culture

Human peripheral blood mononuclear cells (PBMCs) were provided as buffy coats from the Australian Red Cross; NK cells were isolated using a negative selection kit (Stemcell). NK cells were maintained in RPMI with 10% heat-inactivated foetal calf serum and 100 U/ml IL-2 (Peprotech) for 48 h prior to use in mass spectrometry experiments.

KHYG1 cells gene deletion and transduction

The human NK cell line KHYG1 [26] was maintained in RPM1 with 450 U/ml IL-2. HEK293T cells were calcium phosphate transfected with second-generation lentiviral packaging vectors, pFH1tUTG vector (Addgene #70183) encoding doxycycline-inducible sgRNA 5′-TCCCGATGCTACGAGCCGCATCCC-3′, and FUCas9Cherry (Addgene #70182) encoding Cas9 protein. After Retronectin (Takakara)-mediated transduction, guide expression was induced in transduced KHYG1 cells for 7 days, following which GFP$^+$Cherry$^+$ single cell clones were isolated using FACS. The ablation of perforin expression and cytotoxicity was confirmed by Western immunoblot and ^{51}Cr-release assay, respectively. In addition, sequencing of *PRF1* gene revealed an out-of-frame gene disruption at c.359 (Fig EV2). KHYG1 cells were subsequently transduced with HEK293T cell-derived amphoteric virus encoding wild-type or mutant perforin cDNA.

Perforin immunoprecipitation

Protein lysates from $100–200 \times 10^6$ KHYG1 cells or $3–10 \times 10^6$ primary human NK cell were incubated for 2 h with 20 µg of δG9 anti-perforin antibody (eBiosciences) and 40 µl of Protein G bead slurry (GE Healthcare). Unbound protein was washed from beads with lysis buffer following which perforin was eluted with 6 M

Figure 5. Mechanism of cytotoxic lymphocytes protection from perforin.
(1) Within the ER, perforin acquires high-mannose (simple) glycosylation. The C-terminal glycan at residue Asn549 inhibits oligomerisation and thus protects the cytotoxic lymphocyte. Conversely, due to the neutral pH and high Ca^{2+} concentration in the ER, non-glycosylated or partially glycosylated perforin remains active and can kill the host cell [19]. (2) Perforin is rapidly exported from the ER to the Golgi apparatus; this process is critically reliant on the C-terminal residues, particularly the final residue Trp555. Within the Golgi apparatus, high-mannose glycans are replaced with complex glycans. (3) Within secretory lysosomes, low pH renders perforin inactive [13]. Here, the inhibitory glycan is removed through processing of the C-terminus, involving multiple proteases and/or carboxypeptidases. (4) Now active, processed perforin is secreted from the cytotoxic lymphocyte to the membrane of the target cell, where it forms pores.

the molecule. While it is tempting to suggest that carboxypeptidases alone are responsible for proteolysis of perforin, it is unlikely that such an enzyme could process glycosylated Asn549. It is therefore likely that C-terminal cleavage also involves either

guanidine hydrochloride. Following chloroform/methanol precipitation, perforin was deglycosylated using PNGase F (New England Biolabs) as per the manufacturer's instruction and reduced with 50 mM DTT.

Mass spectrometry

For analysis of intact proteins, the complete immune-precipitated mixture in 2% formic acid was separated by reversed-phase chromatography coupled to an ESI-TOF mass spectrometer. All analyses were done on an Agilent 6220 ESI-TOF mass spectrometer coupled to an Agilent 1200 chromatography system (Agilent, CA, USA). Chromatographic separation was performed on a Phenomenex Aeris Widepore-C4 column (2.1 × 150 mm, 3.6 μm bead) at a flow rate of 250 μl/min in the presence of 0.1% formic acid, using a gradient of acetonitrile for elution. All mass spectrometry data were acquired in positive-ion mode and reference mass corrected via a dual-spray electrospray ionisation (ESI) source using a scan range of 100–3,200 m/z, capillary voltage of 4,000 V, fragmentor voltage 250 V, skimmer voltage 65 V, OCT RFV 250 V. Internal reference ions were 121.050873 and 922.009798 m/z. Mass spectra were created by averaging the scans across each peak and background subtracted against the first 10 s of the total ion current. Acquisition was performed using the Agilent Mass Hunter Acquisition software version B.02.01 (B2116.30).

Analysis was performed using Mass Hunter version B.04.00. Perforin typically eluted from the chromatography as a peak at 21.5 min, and the ion spectrum of the peak was de-convoluted to establish the molecular species present. To normalise the traces, given that the overall yields in different experiments varied greatly, the highest peak in each de-convoluted trace was set to a value of one. Peaks present in the de-convoluted trace were assigned as potential perforin fragments (either as N- or C-terminal processing, though no N-terminal processing was evident). Most peaks could be assigned as C-terminally processed perforin. Other minor peaks were either due to other proteins in low abundance, or, for some peaks, assigned as modified versions of perforin. For instance, the shoulder peak visible on the abundant peaks most likely can be attributed to oxidised methionine (plus 16 Da), a modification common in LC-MS. We commonly observed various minor peaks 265–268 Da larger than the major perforin peaks, likely dodecyl sulphate adducts of the protein (from SDS), a phenomenon previously reported [27]. SDS is used in the denaturation of perforin for deglycosylation.

Western immunoblot

Protein lysates were boiled and resolved in Laemmli sample buffer under non-reducing conditions using 9–10% acrylamide SDS–PAGE and transferred to PVDF membrane (Millipore). Perforin was detected using the rat anti-perforin P1-8 antibody (Kyowa Kirin) and HRP-conjugated secondary antibodies. Chemiluminescent signal was detected using X-ray film or Gel-Doc imaging (Bio-Rad).

Inhibition of perforin processing

KHYG1 cells at a cell density of 5×10^5 cells/ml were treated with 25 ng/ml CNCA (Sigma) or 20 μM E64D (Enzo) for 17 h prior to analysis described in text.

Immobilised-metal affinity chromatography (IMAC) enrichment of perforin

Perforin was enriched from KHYG1 cells as previously described [28]. Briefly, $100–300 \times 10^6$ KHYG1 cells were lysed, nuclei were centrifuged at 15,000 *g*, and the clarified supernatant was incubated with Talon cobalt metal affinity resin (Clontech) at 4°C for 1 h. The resin was washed six times with 50 mM Tris and 300 mM NaCl (pH 8.0), and the bound protein was eluted with 270 mM imidazole, 300 mM NaCl and 20 mM Tris (pH 8).

Chromium-release assays

K562 target cells were labelled with 50 μCi $Na_2{}^{51}CrO_4$ (PerkinElmer) for 1 h at 37°C and washed three times to remove excess ^{51}Cr. ^{51}Cr-labelled K562 cells were incubated with IMAC-enriched perforin for 1 h. The cells were then centrifuged, and the radioactivity in the supernatant measured using gamma-counter. Incubation of ^{51}Cr-labelled target cells in medium alone or in 1% Triton X-100 was used to determine the spontaneous and total release, respectively. % specific ^{51}Cr release was calculated as follows: [(test ^{51}Cr release – spontaneous ^{51}Cr release)/(total ^{51}Cr release – spontaneous ^{51}Cr release) × 100]. Chromium release was plotted against relative protein concentrations, as assessed by Western immunoblotting performed concurrently with each experiment. Perforin immunoblot intensities were quantified using ImageJ software.

Oligomerisation and membrane binding assays

Assays were performed as previously described [4]. Briefly, equal amounts of enriched perforin (as determined by Western immunoblot analysis) were incubated with sheep red blood cells in the presence or absence of 1 mM $CaCl_2$ on ice for 2 min. For oligomerisation assays, perforin was incubated with cells for 20 min at 37°C. Cell pellets were resuspended in Laemmli buffer with or without 8 M urea. Samples were then resolved on SDS–PAGE and Western immunoblotting performed as described above.

Comparison of cytotoxic function

To compare the cytotoxicity of perforin isolated from DMSO- or E64D-treated cells, data collected from ^{51}Cr-release assays were normalised by assigning the maximal level of "% specific lysis" observed for each experiment as 100% lysis. Michaelis–Menten plots were fitted using GraphPad Prism software and used to calculate the relative amount of perforin required to achieve 50% lysis. The difference between the two values attained was considered percentage reduction in function.

Glycosidase studies

Enriched perforin was deglycosylated or modified for 20 min with 5 μg of Endoglycosidase H (EndoH), Peptide-N-Glycosidase F (PNGaseF; New England Biolabs, MA, USA) or α2-3,6,8 neuraminidase (New England Biolabs, MA, USA) in IMAC elution buffer. As control, perforin was incubated under the same conditions, but without glycosidases. Deglycosylation was verified by the Western

immunoblotting. Deglycosylated perforin was then used in ^{51}Cr-release assays as described above.

Expanded View for this article is available online.

Author contributions
IGH, CMH and IV designed and conducted the study and co-wrote the manuscript; OG and MAD produced and provided critical reagents; AJB, JCW and RHPL provided input on study design; JAT provided input on study design and co-wrote the manuscript.

Conflict of interest
The authors declare that they have no conflict of interest.

References

1. Podack ER, Young JD, Cohn ZA (1985) Isolation and biochemical and functional characterization of perforin 1 from cytolytic T-cell granules. *Proc Natl Acad Sci USA* 82: 8629–8633
2. Masson D, Tschopp J (1987) A family of serine esterases in lytic granules of cytolytic T lymphocytes. *Cell* 49: 679–685
3. Stinchcombe JC, Majorovits E, Bossi G, Fuller S, Griffiths GM (2006) Centrosome polarization delivers secretory granules to the immunological synapse. *Nature* 443: 462–465
4. Baran K, Dunstone M, Chia J, Ciccone A, Browne KA, Clarke CJP, Lukoyanova N, Saibil H, Whisstock JC, Voskoboinik I *et al* (2009) The molecular basis for perforin oligomerization and transmembrane pore assembly. *Immunity* 30: 684–695
5. Voskoboinik I, Whisstock JC, Trapani JA (2015) Perforin and granzymes: function, dysfunction and human pathology. *Nat Rev Immunol* 15: 388–400
6. Stepp SE, Dufourcq-Lagelouse R, Le Deist F, Bhawan S, Certain S, Mathew PA, Henter JI, Bennett M, Fischer A, de Saint Basile G (1999) Perforin gene defects in familial hemophagocytic lymphohistiocytosis. *Science* 286: 1957–1959
7. de Saint Basile G, Ménasché G, Fischer A (2010) Molecular mechanisms of biogenesis and exocytosis of cytotoxic granules. *Nat Rev Immunol* 10: 568–579
8. Janka GE (2012) Familial and acquired hemophagocytic lymphohistiocytosis. *Annu Rev Med* 63: 233–246
9. Smyth MJ, McGuire MJ, Thia KY (1995) Expression of recombinant human granzyme B. A processing and activation role for dipeptidyl peptidase I. *J Immunol* 154: 6299–6305
10. Pham CTN, Ley TJ (1999) Dipeptidyl peptidase I is required for the processing and activation of granzymes A and B *in vivo*. *Proc Natl Acad Sci USA* 96: 8627–8632
11. Sutton VR, Waterhouse NJ, Browne KA, Sedelies K, Ciccone A, Anthony D, Koskinen A, Mullbacher A, Trapani JA (2007) Residual active granzyme B in cathepsin C–null lymphocytes is sufficient for perforin-dependent target cell apoptosis. *J Cell Biol* 176: 425–433
12. D'Angelo ME, Bird PI, Peters C, Reinheckel T, Trapani JA, Sutton VR (2010) Cathepsin H is an additional convertase of pro-granzyme B. *J Biol Chem* 285: 20514–20519
13. Lopez JA, Susanto O, Jenkins MR, Lukoyanova N, Sutton VR, Law RHP, Johnston A, Bird CH, Bird PI, Whisstock JC *et al* (2013) Perforin forms transient pores on the target cell plasma membrane to facilitate rapid access of granzymes during killer cell attack. *Blood* 121: 2659–2668
14. Metkar SS, Wang B, Aguilar-Santelises M, Raja SM, Uhlin-Hansen L, Podack E, Trapani JA, Froelich CJ (2002) Cytotoxic cell granule-mediated apoptosis: perforin delivers granzyme B-serglycin complexes into target cells without plasma membrane pore formation. *Immunity* 16: 417–428
15. Sutton VR, Brennan AJ, Ellis S, Danne J, Thia K, Jenkins MR, Voskoboinik I, Pejler G, Johnstone RW, Andrews DM *et al* (2016) Serglycin determines secretory granule repertoire and regulates natural killer cell and cytotoxic T lymphocyte cytotoxicity. *FEBS J* 283: 947–961
16. Uellner R, Zvelebil MJ, Hopkins J, Jones J, MacDougall LK, Morgan BP, Podack E, Waterfield MD, Griffiths GM (1997) Perforin is activated by a proteolytic cleavage during biosynthesis which reveals a phospholipid-binding C2 domain. *EMBO J* 16: 7287–7296
17. Law RHP, Lukoyanova N, Voskoboinik I, Caradoc-Davies TT, Baran K, Dunstone MA, D'Angelo ME, Orlova EV, Coulibaly F, Verschoor S *et al* (2010) The structural basis for membrane binding and pore formation by lymphocyte perforin. *Nature* 468: 447–451
18. Lopez JA, Brennan AJ, Whisstock JC, Voskoboinik I, Trapani JA (2012) Protecting a serial killer: pathways for perforin trafficking and self-defence ensure sequential target cell death. *Trends Immunol* 33: 406–412
19. Brennan AJ, Chia J, Browne KA, Ciccone A, Ellis S, Lopez JA, Susanto O, Verschoor S, Yagita H, Whisstock JC *et al* (2011) Protection from endogenous perforin: glycans and the C terminus regulate exocytic trafficking in cytotoxic lymphocytes. *Immunity* 34: 879–892
20. Voskoboinik I, Thia M-C, Fletcher J, Ciccone A, Browne KA, Smyth MJ, Trapani JA (2005) Calcium-dependent plasma membrane binding and cell lysis by perforin are mediated through its C2 domain: a critical role for aspartate residues 429, 435, 483, and 485 but not 491. *J Biol Chem* 280: 8426–8434
21. Shi X, Jarvis DL (2007) Protein N-glycosylation in the baculovirus-insect cell system. *Curr Drug Targets* 8: 1116–1125
22. Moremen KW, Tiemeyer M, Nairn AV (2012) Vertebrate protein glycosylation: diversity, synthesis and function. *Nat Rev Mol Cell Biol* 13: 448–462
23. Sellman BR, Tweten RK (1997) The propeptide of *Clostridium septicum* alpha toxin functions as an intramolecular chaperone and is a potent inhibitor of alpha toxin-dependent cytolysis. *Mol Microbiol* 25: 429–440
24. Iacovache I, Degiacomi MT, Pernot L, Ho S, Schiltz M, Dal Peraro M, van der Goot FG (2011) Dual chaperone role of the C-terminal propeptide in folding and oligomerization of the pore-forming toxin aerolysin. *PLoS Pathog* 7: e1002135
25. Konjar Š, Sutton VR, Hoves S, Repnik U, Yagita H, Reinheckel T, Peters C, Turk V, Turk B, Trapani JA *et al* (2010) Human and mouse perforin are processed in part through cleavage by the lysosomal cysteine proteinase cathepsin L. *Immunology* 131: 257–267
26. Yagita M, Huang CL, Umehara H, Matsuo Y, Tabata R, Miyake M, Konaka Y, Takatsuki K (2000) A novel natural killer cell line (KHYG-1) from a patient with aggressive natural killer cell leukemia carrying a p53 point mutation. *Leukemia* 14: 922–930
27. Fridriksson EK, Baird B, McLafferty FW (1999) Electrospray mass spectra from protein electroeluted from sodium dodecylsulfate polyacrylamide gel electrophoresis gels. *J Am Soc Mass Spectrom* 10: 453–455
28. Froelich CJ, Turbov J, Hanna W (1996) Human perforin: rapid enrichment by immobilized metal affinity chromatography (IMAC) for whole cell cytotoxicity assays. *Biochem Biophys Res Comm* 229: 44–49